

POEMMA: Probe Of Extreme Multi-Messenger Astrophysics

John Krizmanic^{1,2,*} for the POEMMA collaboration[†]

¹CRESST/NASA/GSFC

²University of Maryland, Baltimore County, Baltimore Maryland 21250 USA

Abstract. Developed as a NASA Astrophysics Probe mission concept study, the Probe Of Extreme Multi-Messenger Astrophysics (POEMMA) science goals are to identify the sources of ultra-high energy cosmic rays (UHECRs) and to observe cosmic neutrinos above 20 PeV. POEMMA consists of two satellites flying in loose formation at 525 km altitudes. A novel focal plane design is optimized to observe the UV air fluorescence signal from extensive air showers (EASs) in a stereoscopic UHECR observation mode and the Cherenkov signals from EASs from UHECRs and neutrino-induced τ -leptons in an Earth-limb viewing mode. POEMMA is designed to achieve full-sky coverage and significantly higher sensitivity to the highest energy cosmic messengers compared to what have been achieved so far by ground-based experiments. POEMMA will measure the spectrum, composition, and full sky distribution of the UHECRs above 30 EeV to identify the most energetic cosmic accelerators in the universe and study the acceleration mechanism(s). POEMMA will also have sensitivity to cosmic neutrinos by observing the upward-moving air showers induced from tau neutrino interactions in the Earth. POEMMA will also be able to re-orient to a Target-of-Opportunity (ToO) neutrino mode to view transient astrophysical sources with unique sensitivity. This paper discusses the science goals, instrument design, mission profile, and the simulated UHECR and neutrino measurement capabilities for POEMMA.

1 Introduction

The Probe Of Extreme Multi-Messenger Astrophysics (POEMMA) [1] is designed to use space-based observations of UHECRs and cosmic neutrinos to achieve significant increases in exposure for these messengers of extreme astrophysical phenomena. POEMMA goal is to provide an order of magnitude increase in UHECR exposure in an experimental framework that also provides excellent angular, energy, and nuclear composition resolution for $E_{CR} \gtrsim 30$ EeV and with full-sky coverage of the celestial sphere. POEMMA's UHECR exposure in comparison to past and current ground-based experiments [2–5] is shown in figure 1. POEMMA is also optimized to measure the tau neutrino flux using the optical Cherenkov signals from upward EASs initiated by τ -leptons produced by ν_τ interacting in the Earth with significant sensitivity for $E_\nu \gtrsim 20$ PeV. These measurements are obtained by operating in two different orientation modes using POEMMA's two orbiting Schmidt telescopes, which fly in a loose formation: a quasi-nadir stereo UHECR configuration and a tilted, Earth-limb viewing neutrino configuration. Note that the neutrino mode allows for simultaneous UHECR measurements to occur and with an enhanced geometry factor for the highest energy UHECRs. The POEMMA design leverages previous space-based UHECR and very-high energy (VHE) neutrino mission development, including the OWL study [6], JEM-EUSO [7], EUSO-SPB1 [8], EUSO-SPB2 [9] development, and the CHANT study [10].

*e-mail: john.f.krizmanic@nasa.gov

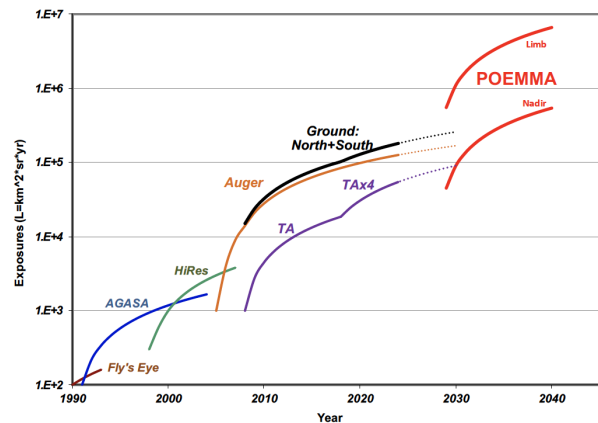


Figure 1. POEMMA's expected exposure growth as compared to past and current ground-based UHECR experiments.

POEMMA was selected by NASA as one of the several concept study proposals to provide science community input for a new class of NASA missions, called Astrophysics Probes [11], to be provided to the 2020 Astronomy and Astrophysics Decadal Survey in support of the development of a recommended portfolio of future astrophysics missions. The Astrophysics Probe mission concepts were funded for 18 month studies, including week-long dedicated engineering study runs. The POEMMA study was performed at the Instrument Design Lab (IDL) and the Mission Design Lab (MDL) in the Integrated Design Center (IDC) [12] at NASA/GSFC. The probe stud-

ies were development with specific instructions to define this unique NASA Class B mission, including Phase A start date (1-Oct-2023) and launch date (1-Nov-2029), launch vehicle guidance, etc., with a total lifecycle (NASA Phases A through E) costs between \sim \$400M and \$1B in FY2018 dollars. In this context, POEMMA is considered as a *potential* probe mission in terms of the 2020 astrophysics decadal review assessment of the probe-class concept. Thus the realization of the probe class depends on the review and NASA's implementation.

As with other NASA probe studies, a detailed report regarding POEMMA will be submitted to NASA. A detailed white paper will also be submitted for publication. In these conference proceedings, an overview of the POEMMA instruments, mission, and simulated UHECR and cosmic neutrino measurement capabilities are presented.

2 Instrument Design

Each POEMMA instrument is comprised of a $f/0.64$ Schmidt telescope using a 4 meter diameter monolithic primary mirror, a 3.3 meter diameter corrector lens, and a 1.6 meter diameter focal plane. A schematic of a deployed telescope with the light doors open and the light shield cut away to show the telescope optics is shown in figure 2. Not shown in the figure is an IR camera, used for cloud measurements, located slightly above the center of the corrector lens and calibration LEDs, used for telescope alignment verification, that are located slightly underneath the outside edge of the corrector lens. Each POEMMA Schmidt telescope has a full Field-of-View (FoV) of 45° , an on-axis effective area of nearly 6 m^2 falling to $\sim 2 \text{ m}^2$ at the edge of the FoV, and fine pixel angular resolution of 0.084° . The point-spread-function (PSF) of the POEMMA optics provide an RMS diameter over the entire FoV that is at most no more than the 3 mm spatial linear pixel size of the photodetectors in the focal plane. The effective area and the UV rms radius as a function of viewing angle are shown in Figure 3.

The focal plane in each POEMMA telescope is dividing into two regions, denoted as the POEMMA Fluorescence Camera (PFC) and the POEMMA Cherenkov Camera (PCC). The PFC optimized for UHECR EAS air fluorescence measurements while the PCC is optimized for the measurement of Cherenkov signals generated by EASs. The majority of the area using Photo Detector Modules (PDMs) based on the JEM-EUSO instrument development [13] for UHECR detection. A smaller segment of the focal plane employs modules consisting of silicon photomultipliers (SiPMs), whose broader wavelength response is better tuned to Cherenkov light measurement, as well as silicon PIN diodes located underneath used to reject the background experienced in low Earth orbit, such as that from cosmic rays. The SiPM focal plane segment is sized to measure Cherenkov signals up to 9° away from the edge of the FoV of a telescope. Figure 4 details the layout of the PFC and PCC in a POEMMA focal plane. The portion of the focal plane for UV air fluorescence detection consists of 55 PDMs, or $126,720 \text{ } 3 \times 3 \text{ mm}^2$ pixels and will record signals using $1 \mu\text{sec}$ temporal sampling. The Cherenkov

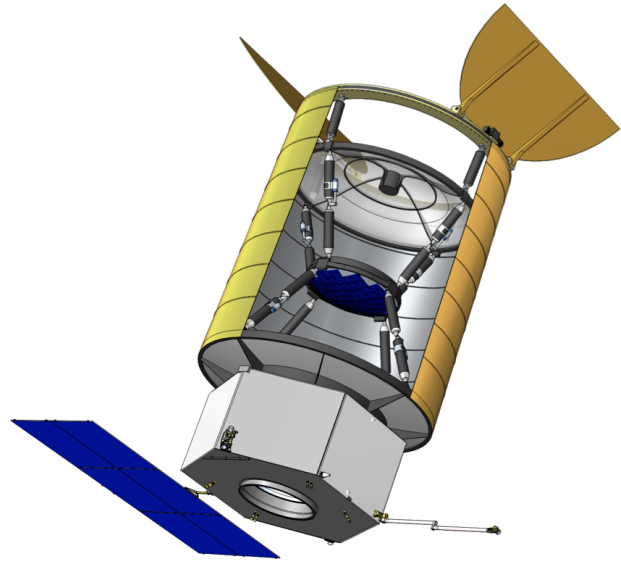


Figure 2. A schematic of a POEMMA Schmidt satellite with the light doors open and with the light shield cut away to show the Schmidt telescope optics.

segment consists of 30 SiPM focal surface units (FSUs), or $15,360 \text{ } 3 \times 3 \text{ mm}^2$ pixels, with custom electronics designed for recording signals using 10 nsec temporal sampling. The front-end electronics for the PDMs and FSUs are located behind the focal plane with signals piped to the data acquisition electronics located underneath the primary mirror and in the satellite bus, the later which includes the avionics, propulsion, power, and communication systems. Table 1 summarizes POEMMA's instrument, spacecraft, and mission specifications.

3 Mission Design

Figure 5 shows a schematic of the stowed POEMMA satellites in a dual manifest Atlas V launch vehicle. The POEMMA monolithic primary mirror was sized such to fit within the diameter constraints of the dual payload adaptor in which the bottom satellite resides. The use of a monolithic primary mirror eliminates the complexity of deploying petals, such as was done in the OWL design [6]. Once in orbit, the payloads will be released and each POEMMA telescope will deploy from its stowed configuration. Initial operations will point the telescopes to the celestial star field to verify the PSF of each POEMMA telescope. After this commissioning phase, the satellites will be arranged in a configuration with $\sim 300 \text{ km}$ satellite separation to perform stereo UHECR measurements then with a satellite separation of $\sim 50 \text{ km}$ to perform neutrino measurements. As the telescopes orbits move them into astronomical night, the light doors open for allow for UHECR or neutrino measurements. The avionics and propulsion of each satellite are designed for orbit maintenance for five years and allow for a fast reorientation between stereo UHECR mode and neutrino mode. For the neutrino mode, this includes a target-of-opportunity (ToO) mode that uses the ability of a POEMMA satellite quickly slew (90° in

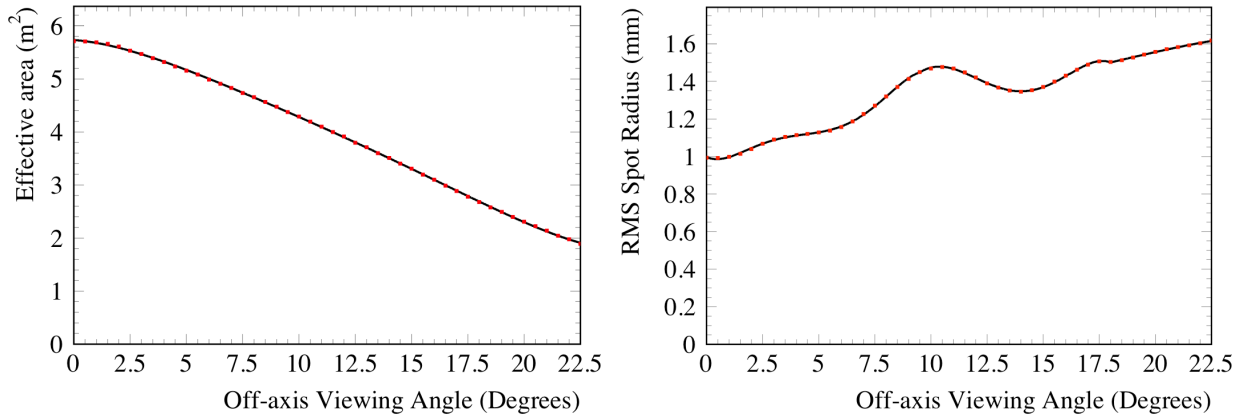


Figure 3. The effective optical collecting area as a function of viewing angle for a POEMMA Schmidt telescope (left) and the rms radius of the UV PSF as a function of viewing angle (right)

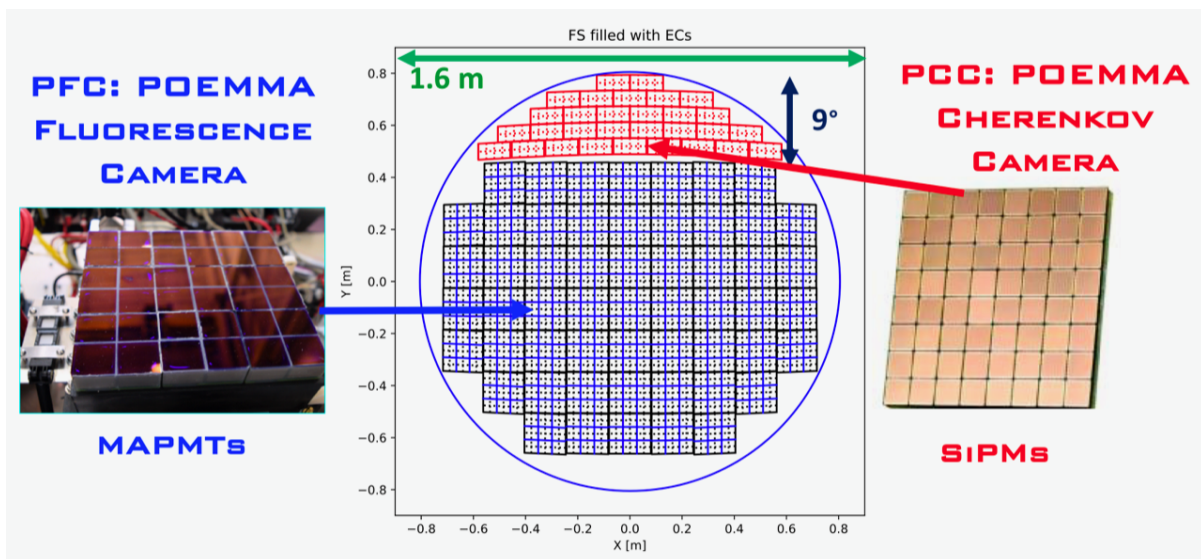


Figure 4. The layout of a POEMMA Schmidt telescope focal plane with PDM and FSU modules. The 9° angular span of the PCC segment is denoted.

a 8 minutes) to observe viewable transient astrophysical events.

3.1 POEMMA Science Operation Modes

Figure 6 illustrates the two POEMMA operational modes. In stereo UHECR mode, the two wide-angle Schmidt telescopes are separated by ~ 300 km and tilted to view a common, immense atmospheric volume (corresponding to approximately 10^{13} tons of atmosphere) to yield a significant yearly UHECR exposure with stereo reconstruction of the UHECR EASs. In the neutrino mode, the POEMMA satellites are separated by ~ 50 km and tilted to view the limb of the Earth (monitoring a terrestrial neutrino target of nearly 10^{10} gigatons, not counting the τ -lepton exit probabilities) and an even more extensive volume of the atmosphere for UHECR fluorescence measurements. As will be discussed later, the smaller satellite separation in neutrino mode is chosen to put both satellites in the EAS Cherenkov light pool to use simultaneous measurements to effectively

lower the EAS Cherenkov threshold to ~ 20 PeV. The baseline neutrino mode has the telescopes tilted 47° away from the nadir such that 2° of the horizon above the Earth limb is viewable to measure the Cherenkov signal from over-the-horizon UHECRs while also viewing the Earth's surface to 7° from the Earth's limb.

4 POEMMA UHECR Response

We have performed initial simulation studies using POEMMA's optical performance to determine POEMMA's UHECR exposure, angular resolution, and nuclear composition (X_{\max}) resolution. For stereo UHECR mode, we chose a satellite configuration with a 300 km separation and with no off-axis tilt angle, as an example. Figure 7 shows the 5 year stereo UHECR exposure, assuming a conservative 10% duty cycle, in terms of 14 years of Auger exposure [14]. Figure 8 shows POEMMA's stereo reconstructed angular resolution, which is $\sim 1^\circ$ or better

Table 1. POEMMA Instrument, Spacecraft, and Mission Specifications

Optics	Schmidt	45° Full FoV
	Primary Mirror	4 meter diameter
	Corrector Lens	3.3 meter diameter
	Focal Surface	1.6 meter diameter
	Pixel Size	3 × 3 mm ²
	Pixel FoV	0.084°
UV Flour. Cherenkov	MAPMT	126,720 pixels
	SiPM	15,360 pixels
Instrument		
	Mass	1,550 kg (each)
	Power	590 W (each)
	Total Data	<1 GB/day
Spacecraft		
	Slew rate	90° in 8 min
	Pointing Res.	0.1°
	Pointing Know.	0.01°
	Clock synch.	10 nsec
	Data Storage	7 days
	Communication	S-band
	Wet Mass	3450 kg
	Total Power	880 W
Mission		
Lifetime	3 year	(5 year goal)
	Orbit	525 km, 28.5° Inc
	Orbit Period	95 min
	Satellite Sep.	~25 - 1000+ km

above 30 EeV, and highlights the strength of the stereo reconstruction technique when one has good pixel angular resolution. The stereo trigger condition in each satellite leads to a highly efficient reconstruction fraction of $\sim 80\%$, with the losses due mainly to the requirement of the $\sim 5^\circ$ opening angle between each EAS geometrical plane. The fine angular resolution leads to highly accurate 3-dimensional EAS reconstruction to provide an energy resolution of $\sim 20\%$ and X_{\max} resolution of potentially $\sim 20 \text{ g/cm}^2$ above $\sim 50 \text{ EeV}$, initially based on an evaluation of the simulated EAS observed photo-electron statistics. This X_{\max} resolution implies sensitivity to a four-component nuclear composition model assuming sufficient event statistics [15]. In addition, if *hot-spots* in the sky are observed with more than 20 events, POEMMA will be able to discriminate the nuclear composition by studying the evolution of the *hot-spot* shape with energy [16]. The UHECR energy threshold is set by brightness of the EASs with respect dark-sky, air glow background in the EAS fluorescence band of $300 < \lambda/\text{nm} < 500$, which is constrained by a near UV filter over the MAPMTs in the focal plane. This combined with the $\sim 6 \text{ m}^2$ optical aperture of each POEMMA instrument yields an UHECR energy threshold of $\sim 30 \text{ EeV}$.

When POEMMA is operating in neutrino mode, the two satellites are separated by $\sim 50 \text{ km}$ and tilted 47° away from nadir to view the limb of the Earth. Consequently, the UHECR asymptotic aperture increases by nearly an order of magnitude, albeit with a higher UHECR energy

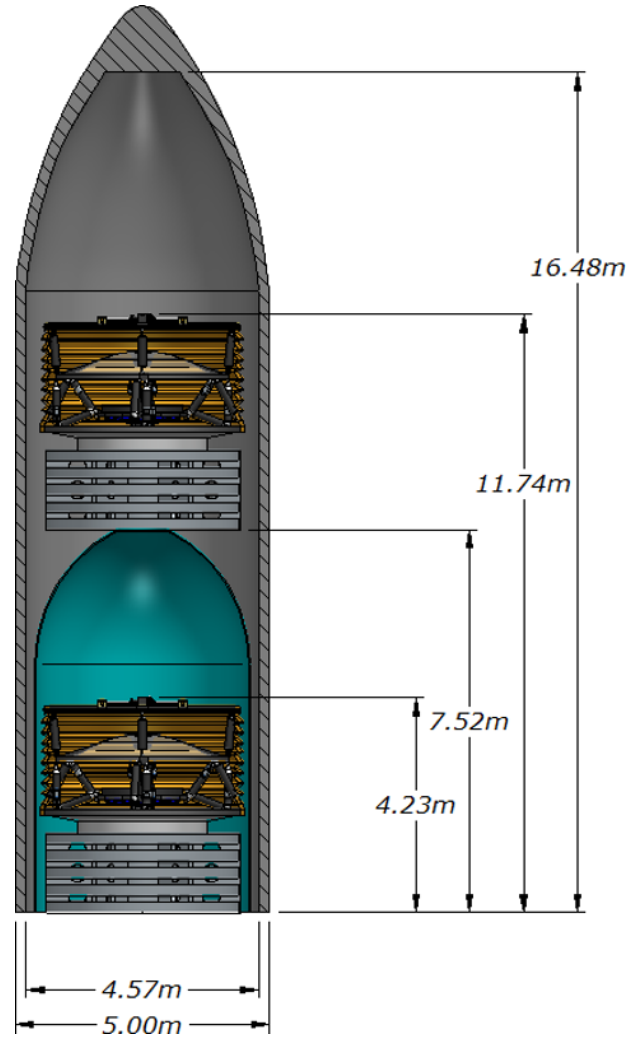


Figure 5. A schematic of the POEMMA satellites in a stowed configuration in dual manifest Atlas V launch vehicle.

threshold for reconstructing the observed events. With the smaller satellite separation, the performance is closer to monocular reconstruction. The ESAF simulation [17, 18] was modified to include the POEMMA optics response (see figure 3) and POEMMA orbit. While the monocular performance in terms of angular (few degree resolution near 100 EeV) and composition ($X_{\max} \sim 100 \text{ g/cm}^2$) resolution is not as good as that for stereo UHECR mode, the energy resolution is still $\sim 20\%$ which allows for the probing of a post-GZK recovery in the UHECR spectrum above 100 EeV, with the enhance exposure due to the tilting (see figure 1). POEMMA is designed to be able to perform both stereo and monocular reconstruction, with the latter being also needed for risk mitigation in the case that one satellite fails to perform properly.

POEMMA has full-sky coverage for UHECR sources due to the nature of the 525 km, 28.5° inclination orbit and large, 45° full FoV for each telescope. A one-year celestial exposure map is shown in figure 9, which shows $\sim 50\%$ variation in the uniformity of the UHECR sky exposure assuming an isotropic flux and no UHECR selection bias. Thus, POEMMA is sensitive to UHECR sources

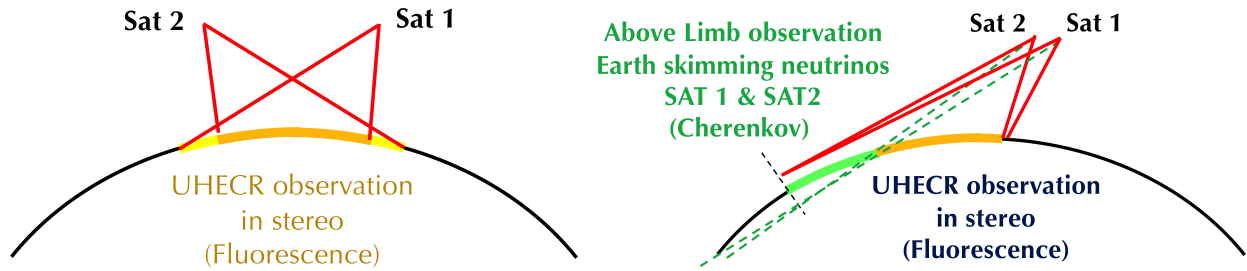


Figure 6. An illustration of POEMMA's stereo UHECR (left) and neutrino (right) observation modes.

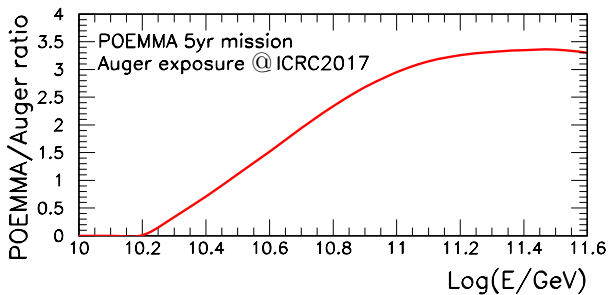


Figure 7. The 5 year POEMMA stereo UHECR exposure for a satellite separation of 300 km, assuming a 10% duty cycle, in terms of 14 years of Auger exposure [14]. From Ref. [16].

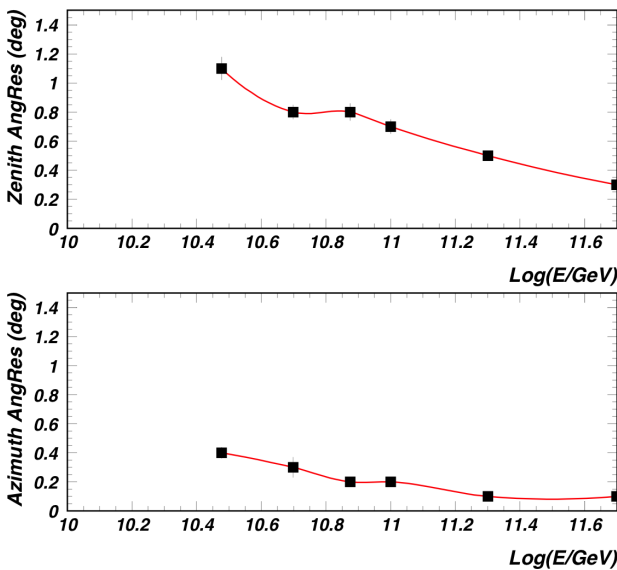


Figure 8. POEMMA's simulated stereo-reconstructed angular resolution versus UHECR energy.

in both the northern and southern hemisphere. POEMMA will measure the UHECR source distribution on the full celestial sphere under a single experimental framework with a well-defined UHECR acceptance, mitigating the issues of cross-comparisons inherent to viewing different portions of the sky with multiple experiments. The ability of the space-based POEMMA telescopes to tilt towards the northern or southern hemisphere allows for the sky expo-

sure can be enhanced for a specific hemisphere to tailor the UHECR sky coverage if desired.

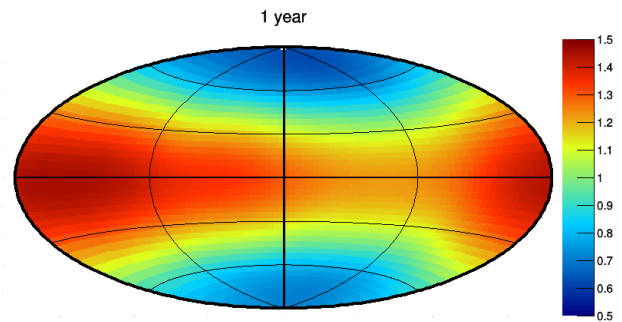


Figure 9. POEMMA's UHECR sky exposure, in declination versus right ascension for one year with the color scale denoting the exposure variations in terms of the mean response. The calculation takes into account the effects of the sun and moon on the duty cycle for observations as well as the eccentricity of the Earth's solar orbit.

5 POEMMA Neutrino Response

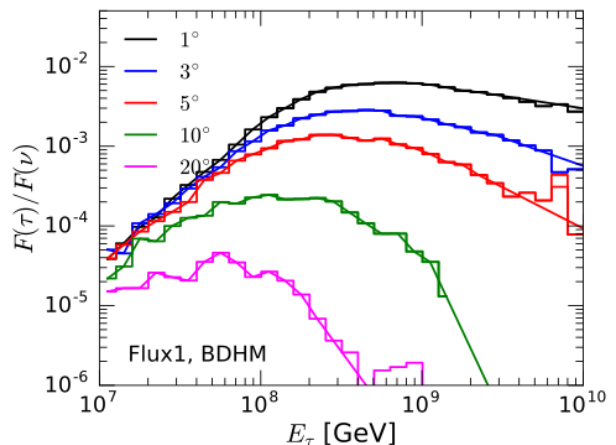


Figure 10. The fractional yield of τ -leptons compared to cosmogenic neutrino energy as a function of energy and Earth emergence angle assuming a mixed nuclear composition UHECR flux from [19]. From Ref. [20]

For neutrinos, POEMMA is optimized for the detection of the EAS Cherenkov light from decays of Earth-

emerging τ -leptons sourced from tau neutrino interactions in the Earth with the use of the FSUs in the focal plane. Figure 10 shows the Earth emerging τ -lepton fraction as a function of energy and Earth emergence angle based on a new calculation developed under the POEMMA probe study [20]. The figure shows the effect of the different column depths, which increases as the Earth emergence angle increases, on the energy spectrum of emerging τ -leptons and the neutrino energy sensitivity. Due to the neutrino cross section increasing with energy [21], smaller column depths provide sensitivity to higher energy neutrinos. Longer column depths are sensitive to lower energy neutrinos, but with a component due to tau neutrino regeneration [22]. Simulation studies have indicated that POEMMA's sensitivity for tau neutrinos below 100 PeV is dominated for Earth emergence angles larger than 10° , corresponding to viewing angles larger than 2° away from the limb. POEMMA will view the Earth 7° away from the limb, or $\sim 20^\circ$ in Earth emergence angle, in order to be enhance the sensitivity to tau neutrinos below 100 PeV. POEMMA will also look 2° above the limb to measure any over-the-horizon backgrounds from UHECR Cherenkov signals [23]. The results of upward-moving EAS simulations shown in figure 11 indicate that the Cherenkov light profile at POEMMA is essentially a flat top with a spatial width at 525 km of 10's of km and with a power law-falloff. This motivates the satellite separation for neutrino mode to be $\lesssim 50$ km in order to have a high probability that both satellites are in a significant portion of the light pool, basically viewing the Cherenkov signal is one pixel, albeit with some spread due to the PSF of the optics.

Figure 11 also presents the spectrum of Cherenkov light delivered to a POEMMA telescope for a 100 PeV EAS with a 10° Earth emergence angle initiated at sea level. Both the Cherenkov intensity and spectrum vary depending on the the interplay between the τ -lepton Earth-emergence angle, τ -lepton energy (and hence decay altitude), the Cherenkov light generation and atmospheric absorption, and the result determines the observability of an upward-moving EAS. For example, while figure 10 shows a significant flux of sub-100 PeV τ -leptons for smaller Earth-emergence angles, these decay at very low altitudes and the Cherenkov light gets strongly absorbed by the low-altitude aerosols. Figure 12 illustrates this by examining the Cherenkov intensity and wavelength dependence for a fixed Earth emergence angle and EAS energy as a function of starting altitude. At the lowest altitudes, aerosol absorption decimates the Cherenkov intensity and pushes the spectrum towards the longest wavelengths. However, the exponential nature of both the aerosol layer and atmosphere itself leads to EAS higher Cherenkov intensities and spectra peaked at lower wavelengths fairly quickly as a function of EAS starting altitude. Eventually the atmosphere becomes too rarified for complete EAS development, leading to a reduction in the Cherenkov intensity for EAS developing above ~ 17 km altitudes.

We have used simulations that take into account all these effects to determine the ability for POEMMA to observe the beamed Cherenkov signal over the Cherenkov band $300 < \lambda/\text{nm} < 900$ band to set the energy thresh-

old for Cherenkov observations in POEMMA. Simulations have also shown that the accepted upward τ -lepton induced EAS has a temporal width of ~ 20 ns. This defines the sampling time for the SiPM portion of the focal plane, and using a coincidence window of 60 ns assuming simultaneous observation of using both POEMMA telescopes results in a false positive Cherenkov signal of $\sim 0.1\%$ due to the air glow background in the Cherenkov band ($300 < \lambda/\text{nm} < 900$) and with sensitivity to tau neutrinos down to ~ 20 PeV. This is shown in figure 13 which presents the tau neutrino aperture as a function of incident neutrino energy as calculated by the end-to-end optical Cherenkov simulation of upward, τ -lepton -induced EAS from tau neutrinos interacting in the Earth as measured by POEMMA [20]. For POEMMA, the coincidence timing requirement corresponds to the curve for an azimuth angle range of 30° but the potential of using the full azimuth range of 360° is also presented. The curves show that significant sensitivity to tau neutrinos above $\gtrsim 20$ PeV can be achieved using the optical Cherenkov signal from upward τ -lepton -induced EASs.

POEMMA's exposure for cosmic tau neutrino sources is defined by the instantaneous FoV for the optical Cherenkov signal from EAS, defined by the roughly 9° by 30° span of the SiPM portion of the focal plane. For one orbit period, this Cherenkov FoV traces out a band on the celestial sky defined by the inclination of the orbit and the off-orbit angle the telescopes point. Figure 14 (from Ref. [24]) shows the band in declination versus right ascension defined by POEMMA's FoV for the tau neutrinos interacting in the Earth for one example orbit. Given POEMMA's approximately 90 minute orbit period, it is straightforward to define an observation strategy that make judicious adjustments to pointing direction over many orbits to achieve an effective full-sky coverage for tau neutrino sources. Figure 15 (from Ref. [24]) shows the one year tau neutrino sky coverage, based on an specific set of defined repoints for each orbital period, demonstrating full sky coverage. Again, this illustrates the unique ability of POEMMA to use its inherent ability to repoint to realize the full benefits of space-based observation, e.g. full sky coverage for cosmic neutrino sources. Further optimization of the repoints during the year-long observational period could improve the uniformity of the sky exposure.

5.1 Neutrino Target-of-Opportunity

The ability of the POEMMA satellites to quickly reorient into a neutrino observation mode allows POEMMA to easily move into a ToO neutrino mode once a interesting transient event is detected in another multimessenger band, eg gravity waves or gamma-ray flares. The ability to accept a ToO alert was designed into POEMMA's communication architecture as well as in the avionics to perform the required flight dynamics for the POEMMA telescopes to quickly repoint to a proper orientation. If the source is located in at a point in the sky that is available for viewing through the Earth's limb with a significant τ -lepton induced EAS Cherenkov signal, the POEMMA telescopes can follow the source until it effectively outside the tau

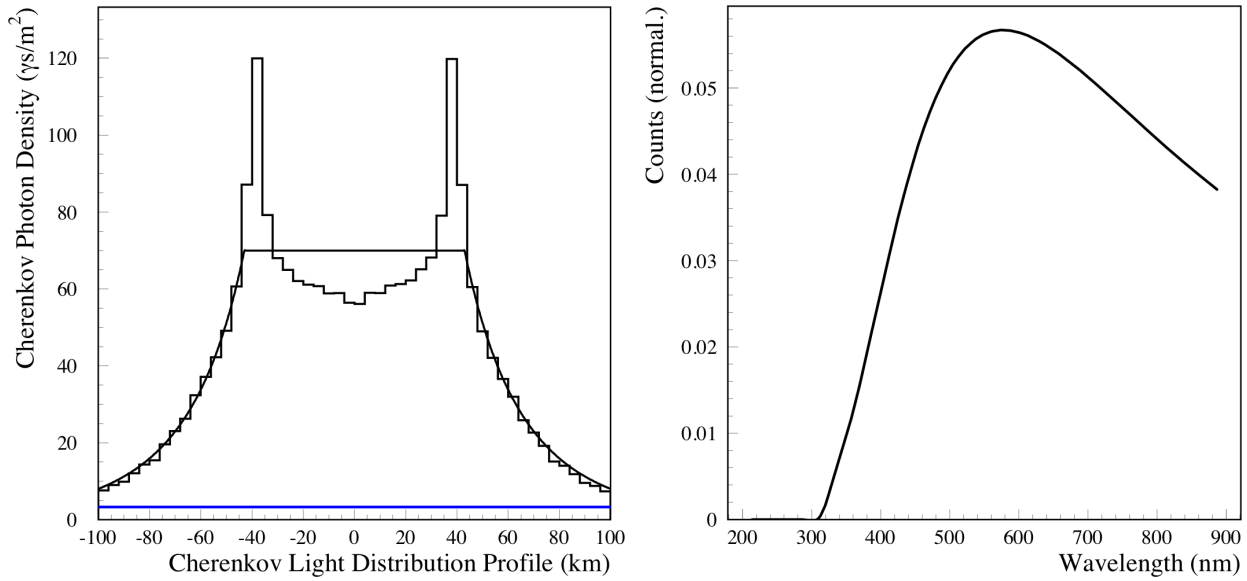


Figure 11. The spatial profile of the Cherenkov signal (photons/m²) at 525 km altitude for a 100 PeV upward EAS with a 10° Earth emergence angle initiated at sea level (left) and the simulated Cherenkov spectrum observed by a POEMMA telescope for the event (right).

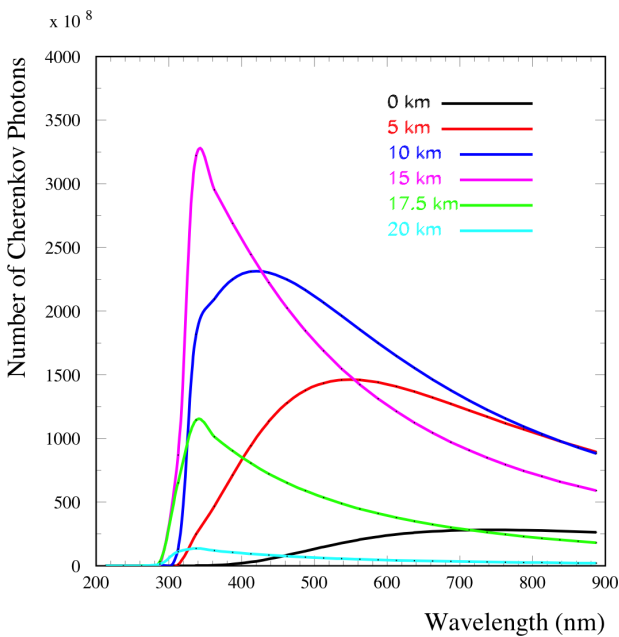


Figure 12. The intensity and wavelength dependence of the Cherenkov signal for 100 PeV upward-moving EASs for 5° Earth emergence angle as a function of EAS starting altitude. From Ref. [20].

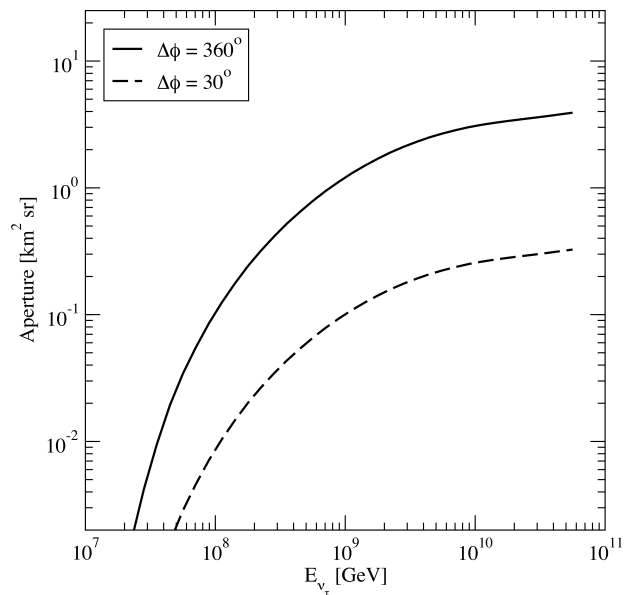


Figure 13. The effective tau neutrino aperture as a function of energy assuming the ability to view an azimuthal range of 30° and 360°. From Ref. [20]

neutrino field of view, which is set by the probability of observing a τ -lepton EAS above ~ 20 PeV for the viewed column depth through the Earth. The source location is smeared by up to a few degrees by the Cherenkov angles of the EAS, but will be well within the $30^\circ \times 9^\circ$ angular span of each POEMMA focal plane optimized for Cherenkov EAS measurement. Some theoretical models of neutron-star mergers, such as the model of Fang and Metzger [25], predict the peak neutrino flux could occur months after the

initial merger. This implies if the source is in part of the celestial sky viewable by POEMMA, the evolution of the neutrino flux can be measured. Alternatively, if the transient source is not currently viewable due to current solar-Earth-source orientation, it could eventually come into POEMMA's neutrino FoV while the neutrino flux is still observable, and exploits the fact that POEMMA's space-based observations have the ability to observe sources with full sky-coverage if they are long enough in duration or have a relatively high rate of occurrence.

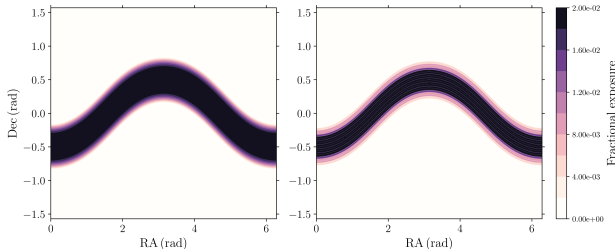


Figure 14. The neutrino sky exposure for one POEMMA orbit in declination versus right ascension, assuming the telescopes are pointed along the orbit trajectory. The rightmost plot shows the exposure assuming the finite extent of the SiPM focal plane modules. From Ref. [24].

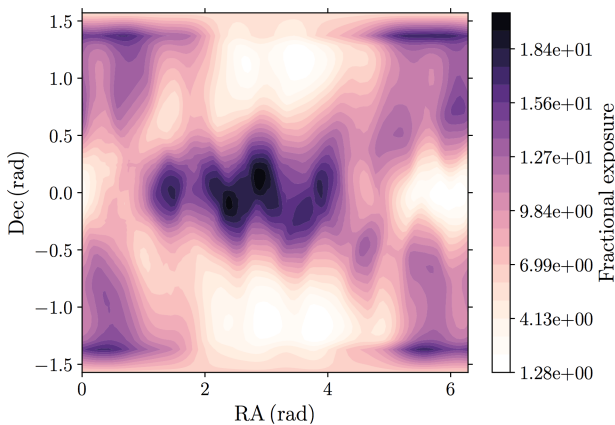


Figure 15. The fractional neutrino sky exposure for one year in declination versus right ascension, assuming a defined variation in the POEMMA limb-pointing directions over the year to achieve full-sky coverage. The calculation takes into account the effects of the sun and moon on the duty cycle for observations. From Ref. [24].

6 Summary and Discussion

POEMMA was developed as a NASA Astrophysics Probe mission concept study, and designed with the science goals are to identify the sources of ultra-high energy cosmic rays (UHECRs) and to observe cosmic neutrinos above 20 PeV. In this paper, the POEMMA instruments, mission, and UHECR and cosmic neutrino measurement performance based initial simulation of the POEMMA probe study design are presented. POEMMA's 5-year stereo UHECR exposure is predicted to be slightly more than that for Auger's 14-year exposure around 30 EeV growing to more than 3 times that around 100 EeV. Initial simulations show 1° or better angular resolution above 50 EeV and initial studies show the potential for X_{\max} resolution around 20 g/cm² using stereo reconstruction. Initial simulations employing monocular reconstruction, close to that anticipated when the POEMMA satellites are tilted towards the limb in neutrino mode, show poorer X_{\max} and angular resolution, but with $\sim 20\%$ energy resolution and larger exposure for the highest energy UHECRs. The tau neutrino simulations developed under the POEMMA study have yielded a baseline end-to-end modeling package that as-

sesses the details of using the Earth as a tau neutrino converter and measuring the Cherenkov light from upward-moving EASs developed from Earth-emergence τ -lepton decays. This simulation was used to quantify the effective tau neutrino aperture for POEMMA as well as showing the potential if the entire azimuth angle range can be observed. The POEMMA tau neutrino aperture is currently being used to assess the potential of POEMMA to make ToO observations of transient events that may have significant neutrino flux, such as neutron star mergers.

The NASA Probe concept studies, including that for POEMMA, are motivated by providing input to the upcoming 2020 Astronomy and Astrophysics Decadal Survey by NASA to evaluate the astrophysics probe mission concept. Thus the current POEMMA probe design can be considered an first design of a UHECR and VHE neutrino probe and can be built upon for an eventual probe once (and if) NASA releases a probe AO in the future. Naturally, POEMMA's performance can be significantly increased by increasing the EAS light collecting ability. Given the UHECR imaging requirements are modest, 1 km from 525 km corresponds to $\sim 0.1^\circ$ or $\gtrsim 10^4$ away from the diffraction limit in the near-UV, the requirements on the optical performance of POEMMA's Schmidt telescopes are closer to that of a microwave dish than a true optical telescope, such as the Hubble Space Telescope. Technology development in the area of lightweight, deployable optical structures, building upon those used in NASA's Inflatable Antenna Experiment (IAE), which included a 14-meter diameter primary, that was deployed in space in 1996 and more recent R&D offer a path to significantly increase the light collection ability space-based UHECR and VHE neutrino experiments.

† **POEMMA Collaboration** A. Olinto¹, J. Adams², R. Aloisio³, L. Anchordoqui⁴, D. Bergman⁵, M. Bertaina⁶, P. Bertone⁷, F. Bisconti⁶, M. Casolino⁸, M. Christl⁷, A. Cummings³, I. De Mitrì³, R. Diesing¹, J. Eser⁹, F. Fenu⁶, C. Guepin¹⁰, E. Hays¹¹, E. Judd¹², J. Krizmanic¹¹, E. Kuznetsov², S. Mackovjak¹³, J. McEnery¹¹, J. Mitchell¹¹, A. Neronov¹⁴, F. Oikonomou¹⁵, A. N. Otte¹⁶, E. Parizot¹⁷, T. Paul⁴, J. Perkins¹¹, G. Prevot¹⁷, P. Reardon², M. H. Reno¹⁸, F. Sarazin⁹, K. Shinozaki⁶, J. Soriano⁴, F. Stecker¹¹, Y. Takizawa⁸, M. Unger¹⁹, T. Venters¹¹, L. Wiencke⁹, R. M. Young²

¹The University of Chicago, Chicago, IL, USA; ²University of Alabama, Huntsville, AL, USA; ³Gran Sasso Science Institute, L'Aquila, Italy; ⁴CUNY, Lehman College, NY, USA; ⁵University of Utah, Salt Lake City, Utah, USA; ⁶Università di Torino, Torino, Italy; ⁷NASA Marshall Space Flight Center, Huntsville, AL, USA; ⁸RIKEN, Wako, Japan; ⁹Colorado School of Mines, Golden, CO, USA; ¹⁰Sorbonne Université, Institut d'Astrophysique de Paris, Paris, France; ¹¹NASA Goddard Space Flight Center, Greenbelt, MD, USA; ¹²Space Sciences Laboratory, University of California, Berkeley, CA, USA; ¹³Institute of Experimental Physics, Slovak Academy of Sciences, Kosice, Slovakia; ¹⁴University of Geneva, Geneva, Switzerland; ¹⁵European Southern Observatory, Garching bei Munchen, Germany; ¹⁶Georgia

Institute of Technology, Atlanta, GA, USA; ¹⁷*APC, Univ Paris Diderot, CNRS/IN2P3, CEA/Irfu, Paris, France;* ¹⁸*University of Iowa, Iowa City, IA, USA.* ¹⁹*Karlsruhe Institute of Technology, Karlsruhe, Germany*

References

- [1] A.V. Olinto et al., ArXiv e-prints (2017), 1708.07599
- [2] J. Abraham et al., Nuclear Instruments and Methods in Physics Research A **613**, 29 (2010), 1111.6764
- [3] J. Abraham et al., Nuclear Instruments and Methods in Physics Research A **620**, 227 (2010)
- [4] T. Abu-Zayyad et al., Nuclear Instruments and Methods in Physics Research A **689**, 87 (2012), 1201.4964
- [5] H. Tokuno et al., Nuclear Instruments and Methods in Physics Research A **676**, 54 (2012), 1201.0002
- [6] F.W. Stecker et al., Nuclear Physics B Proceedings Supplements **136**, 433 (2004), astro-ph/0408162
- [7] J.H. Adams et al. (JEM-EUSO), Astropart. Phys. **44**, 76 (2013), 1305.2478
- [8] L. Wiencke, A. Olinto, Proceedings of the 35th ICRC (Busan) (2017), PoS(ICRC2017)1097.pdf
- [9] J.H. Adams et al., ArXiv e-prints (2017), 1703.04513
- [10] A. Neronov et al., Phys. Rev. **D95**, 023004 (2017), 1606.03629
- [11] NASA Research Announcement Astrophysics Probe Mission Concept Studies, Solicitation: NNH16ZDA001N-APROBES
- [12] See <https://idc.nasa.gov/idc/>
- [13] J.H. Adams, S. Ahmad, J.N. Albert, D. Allard, L. Anchordoqui, V. Andreev, A. Anzalone, Y. Arai, K. Asano, M. Ave Pernas et al., Experimental Astronomy **40**, 19 (2015)
- [14] F. Fenu, Pierre Auger Collaboration, International Cosmic Ray Conference **35**, 486 (2017)
- [15] J. Krizmanic, D. Bergman, P. Sokolsky, arXiv e-prints (2013), 1307.3918
- [16] R.C. dos Anjos, J.F. Soriano, L.A. Anchordoqui, T.C. Paul, D.F. Torres, J.F. Krizmanic, T.A.D. Paglione, R.J. Moncada, F. Sarazin, L. Wiencke et al., Phys. Rev. D **98**, 123018 (2018), 1810.04251
- [17] F. Fenu, T. Mernik, A. Santangelo, K. Shinozaki, M. Bertaina, L. Valore, S. Bitkemerova, D. Naumov, G. Medina Tanco, International Cosmic Ray Conference **3**, 116 (2011)
- [18] F. FENU, International Cosmic Ray Conference **3**, 120 (2011)
- [19] K. Kotera, D. Allard, A.V. Olinto, JCAP **10**, 013 (2010), 1009.1382
- [20] M.H. Reno, J.F. Krizmanic, T. Venters, in preparation (2019)
- [21] M.M. Block, L. Durand, P. Ha, Phys. Rev. **D89**, 094027 (2014), 1404.4530
- [22] F. Halzen, D. Saltzberg, Phys. Rev. Lett. **81**, 4305 (1998), hep-ph/9804354
- [23] A. Neronov, D.V. Semikoz, I. Vovk, R. Mirzoyan, Phys. Rev. D **94**, 123018 (2016)
- [24] C. Guépin, F. Sarazin, J. Krizmanic, J. Loerincs, A. Olinto, A. Piccone, arXiv e-prints (2018), 1812.07596
- [25] K. Fang, B.D. Metzger, ApJ **849**, 153 (2017), 1707.04263